PAPER 60 (SESSION V)

The interactions of deformation processes in high purity aluminium

K. J. MILLER* and M. N. RISK

*Lecturer, The Faculty of Engineering, University of Cambridge.
†Research Assistant, Department of Materials, Queen Mary College, University of London.

Summary

The investigation concerns the interactions of monotonic, cyclic-creep and fatigue processes in high purity aluminium subjected to high torsional strains. Torsion was selected as a method of testing a ductile material in order to apply a constant strain rate over the whole surface of the working section in which cracks are initiated. Specimens were subjected to alternating torque at nine surface strain rates in the range $4{\cdot}8 \times 10^{-4} s^{-1}$ to $286 \times 10^{-4} s^{-1}$, and five temperatures in the range 15°C to 250°C.

Deformation processes include monotonic work-hardening, cyclic strain hardening, cyclic strain softening, stress relaxation, cumulative strain (cyclic-creep) and fatigue. The ratio of time-to-cyclic-dependent deformation, R, is shown to be dependent on the straining rate, torque range, and temperature; R varying from 2 to 35% in this study. By introducing a parameter, γ_t, (the life summation of cyclic creep and fatigue strains) a single curve can describe the behaviour of specimens at a constant temperature irrespective of straining rate. The summation term, which represents the total plastic strain path traversed to failure, may be modified to account for the change in fracture ductility at various temperatures. The correction factor, β, is found to be a function of both temperature and life. An empirical equation is derived in the form

$$N_f^{\alpha} = Ke^{\beta\gamma_t}$$

to satisfy all test results within a scatter of ±4% irrespective of the relative amounts of the various deformation processes.

Introduction

Several investigators [1, 2, 3] have shown that there is a frequency effect in the high strain fatigue behaviour of metals. This effect can be equated to a rate of deformation effect since

$$\text{frequency of cycling} = \frac{\text{straining rate}}{2\Delta\epsilon_t} \qquad (1)$$

where $\Delta\epsilon_t$ is the total strain range. Three recent publications [4, 5, 6] have emphasized that since $\Delta\epsilon_t$ varies throughout a test series it is more desirable to maintain a constant strain rate than a constant frequency of cycling. A recent paper [7] of which this present investigation is an extension

has shown that above a critical strain rate, $\dot{\gamma}_{crit}$ failures are predominantly due to fatigue but at rates $<\dot{\gamma}_{crit}$ time-dependent mechanisms play a significant role in the deformation processes. At the intermediate temperature of $0{\cdot}315T_m$ it was found that the ratio of time-dependent to cyclic-dependent processes was a function of strain rate. Manifestations of the effect of strain rate were

(i) fatigue lives increased as the strain rate increased, and

(ii) cumulative strains increased as the strain rate decreased.

One conclusion of the previous work was that although a variation in the strain rate causes a variation in the degree of interaction between fatigue and cyclic-creep processes a single parameter γ_t appeared to determine the life of specimens.

The parameter γ_t (total plastic deformation) is determined from the equation

$$\gamma_t = \Sigma 2\Delta\gamma_p + \Sigma\Delta\gamma_c \qquad (2)$$

where $\Delta\gamma_p$ is the cyclic plastic strain range

and $\Delta\gamma_c$ is the cyclically-induced-creep component per cycle.

The work described in this paper is an extension of the work in reference [7] and involves a study of the interaction of deformation processes at various strain rates, torque ranges and temperatures in a high purity (99·99%) aluminium.

Materials and specimens

The material used was a high purity aluminium (99·99%) supplied in a single bloom, and then cold drawn to 1 in diameter bars from 3 in square sections. To eliminate strain concentrations and to make a comparative study a similar geometry of specimen was used as in the previous work [7], see Fig. 1. Machining was carried out on a copy lathe and a uniform grain size of 25 grain boundaries per linear millimetre was achieved by a post-machine anneal at 400 °C. Results of monotonic tests to failure in torsion at various temperatures but identical straining rates are given in Fig. 2.

Apparatus and instrumentation

Ten twisting rates within the range 4·4 to 252 degrees/min could be applied to a specimen. The specimen holders were designed to ensure that no axial or bending forces could be applied to the test pieces. A torque bar fitted with strain gauges and a radius arm acted both as a load measuring system and mechanical device to control the torque limits. The method of torque control proved to be simple and reliable with the torque range maintained to within an error of ±0·1% throughout all tests. Automatic strain reversals occurred by the triggering of a relay circuit due to

the torque radius arm touching pre-set limit stops. The switching circuit was designed to operate under all conditions, but particularly at the extremely light contact pressures between the radius arm and the limit switches due to torque sensitivity at high cyclic strain ranges. The angular rotation of one end of the specimen relative to the other was recorded by a transducer driven by a differential pulley system. Signals from the strain gauges and the transducer were fed into an XY pen recorder which plotted hysteresis loops throughout the fatigue life.

Elevated temperatures were achieved by circulating hot air round the specimen which was enclosed in an asbestos jacket. Air was forced into a remote wire-wound furnace by a small centrifugal pump. To ensure a uniform temperature distribution over the entire gauge length, the air circulation was controlled by regulating valves on two separate inlet pipes to the jacket. The temperature variation along the gauge length was maintained to ± 0·5% of the test temperature. A thermocouple was inserted into the shoulder of each specimen to control the furnace via a proportional temperature device. Two other thermocouples were used to record specimen and air temperatures respectively at the working surface. Specimen temperatures were maintained to within ±1% throughout all tests.

Experiments

Some 77 tests, were carried out each test being performed at a constant temperature and rate of twisting within pre-set torque limits of equal but reversed magnitudes. Test temperatures were 20°, 110°, 160°, 205° and 250 °C, and the surface strain rates were 4·8, 9·4, 14·8, 16·9, 32·6, 48·7, 83·6, 160 and $286 \times 10^{-4}\,s^{-1}$. To facilitate comparison of data at different straining rates, several test series were conducted, such that the selected torque range gave approximately the same number of cycles to failure at each of the above mentioned temperatures. Hysteresis loops of torque versus angle of twist were plotted at regular intervals during each test but the angular deformation of the specimen could be visually checked on a protractor scale. Frequency of cycling varied from 3 to 720 c/hr for most tests although the programme involved a few tests operating at 0·3 c/hr. Since the investigation involved both fatigue and cyclically induced creep mechanisms, failure was defined as the instant when complete rupture of the section occurred.

Results and their interpretation

Fatigue endurance data were obtained at all temperatures. Fig. 3 is typical of all the results and indicates that for a given temperature range a decrease in number of cycles to failure occurs as the straining rate decreases although the effect is most marked at very low strain rates. It must be noted however that a decrease in the rate of deformation increases

the life in terms of time to failure. Results from all tests show that for lives in excess of ten cycles a relationship of the form

$$TN_f^a = \text{constant} \tag{3}$$

is applicable but the constant and a are both temperature and strain rate dependent.

Fig. 4 illustrates the typical cumulative strain behaviour of the material and clearly shows that the straining rate influences the secondary and tertiary stages of cyclically-induced creep.

Hysteresis loops

Before proceeding to a discussion of the results, a simplified interpretation of the shape of the various forms of hysteresis loops is presented.

The tests referred to in this paper are basically fatigue tests, although a high proportion of damage can be attributed to cyclically induced creep. To distinguish between the two damaging processes reference is made to a typical hysteresis loop shown in Fig. 5 (a). The cyclic strain range $\Delta\gamma_p$ is the minimum width of the hysteresis loop and is a totally reversed path, consequently this term is closely related to the plastic strain range term $\Delta\epsilon_p$ in the Manson-Coffin high-strain fatigue relationship

$$\Delta\epsilon_p \cdot N_f = \text{constant} \tag{4}$$

As a first order approximation therefore $\Delta\gamma_p$ may be referred to as the 'fatigue' component. The cyclically-induced-creep component, $\Delta\gamma_c$ is the residual strain at the end of each cycle. Summation of this component throughout life gives a curve similar to conventional creep curves, see Fig. 4.

The torque range, $2T$, was kept constant throughout each test thus allowing $\Delta\gamma_c$ to accumulate.

Cyclic softening and cyclic hardening is said to occur if the term $\Delta\gamma_p$ increases or decreases respectively as life progresses. Stress relaxation occurs if there is a negative slope in the loop as at X in Fig. 5 (a). Several tests were performed on tensile specimens of the same material at low strain rates to verify that this effect was indeed a cyclically-induced stress relaxation phenomenon.

The shape of the loop

The loop profile is a function of torque range, straining rate, temperature and life. All these four factors influence the cyclic softening, hardening and stress relaxation processes that occur and in consequence effect the

terms $\Delta\gamma_p$ and $\Delta\gamma_c$. In general the whole investigation may be considered to be sub-divided into four zones; see Fig. 5 (b).

Below the critical torque range, T_{crit}, cyclic hardening occurred at all strain rates but this changes to cyclic softening close to failure, especially at very low strain rates when stress relaxation appeared. At $T > T_{crit}$ cyclic softening always occurred. No reference to this reversal of behaviour can be found in the literature although sometimes the reverse may occur [8] when cyclic softening changes to cyclic hardening at higher load amplitudes.

Above a critical strain range $\dot{\gamma}_{crit}$ there is only a minimal change in fatigue life but below $\dot{\gamma}_{crit}$ time-dependent processes have an important role. The effect of increasing the temperature is to increase the value of $\dot{\gamma}_{crit}$ and decrease the value of T_{crit}.

Zones 1 to 4 may be described as follows.

Zone 1. Initially $\Delta\gamma_p$ and $\Delta\gamma_c$ decrease, i.e. cyclic-strain hardening occurs but this is soon followed by a steady state condition. No stress relaxation occurs but close to failure cyclic softening appears. Failures from this zone are predominantly due to fatigue processes.

Zone 2. No cyclic hardening occurs and both $\Delta\gamma_p$ and $\Delta\gamma_c$ increase throughout life. Minimal stress relaxation occurs in all cycles.

Zone 3. Cyclic hardening occurs but not to the same extent as in Zone 1. The steady state cumulative creep is more pronounced than in Zone 1 and cyclic softening occurs close to failure to an extent that eventually causes stress relaxation.

Zone 4. Cyclic softening and stress relaxation persists from the first cycle. The cyclically-induced-creep component increases rapidly throughout life. Time dependent deformation as symbolised by $\Sigma\Delta\gamma_c$ represents a considerable proportion of the total deformation failure, γ_t.

The influence of time-dependent processes of deformation increases progressively from Zone 1 to Zone 4. This is obvious in that at high torques and low strain rates the material is subjected to near constant forces for greater periods of time.

Discussion

The effect of strain rate on the fatigue life of specimens subjected to a constant torque range is illustrated in Fig. 6. The critical strain rate is not as clearly defined at elevated temperatures but at room temperature $\dot{\gamma}_{crit}$ is the same as that obtained in testing commercially (99%) pure aluminium [7]. The critical strain rate is independent of torque range but dependent on temperature, see Table 1.

It is argued from Fig. 6 that below $\dot{\gamma}_{crit}$ time-dependent processes are important in high-strain fatigue behaviour.

To further illustrate the effect of strain rate on deformation processes Fig. 7 shows the ratio of cumulative strain to the cyclic plastic strain path,

$$R = \frac{\Sigma\Delta\gamma_c}{\Sigma\Delta\gamma_p}$$

as a function of the rate of deformation. At high temperatures and low strain rates a significant proportion of deformation is due to cyclic creep. At strain rates at or about the critical value the ratio R is approximately 8% and temperature appears to have minimal effect on this value.

To study the effect of torque range on the ratio of time to cyclic dependent deformation at various temperatures, it is necessary to compensate the torque range to comparable values, i.e. values related to the monotonic torques at the various temperatures. In consequence, Fig. 8 is plotted on a base of torque range/maximum monotonic torque. The percentage of cumulative strain increases as torque range increases but is temperature insensitive at low torques. At high torques the cumulative strain increases at an increasing rate especially at higher temperatures.

So far the discussion has shown that a family of fatigue-endurance and cyclically-induced-creep curves can be bred by changing the straining rate. In general it was observed that a decrease in the fatigue component indicated an increase in the cyclic-creep component and this led to the investigation of the total plastic strain path to failure, γ_t, as a criterion of failure where

$$\gamma_t = \Sigma\Delta\gamma_c + 2\Sigma\Delta\gamma_p \qquad (2)$$

It may be pointed out that with aluminium subjected to high strain fatigue, the elastic component is negligible in comparison with the plastic component.

Plotting log γ_t against log N_f gives the curves of Fig. 9. It is interesting to note that for any particular temperature a single curve can describe the results of tests irrespective of (i) cyclic hardening, cyclic softening, or stress relaxation and (ii) the ratio $\Delta\gamma_c : \Delta\gamma_p$. This was also found in the case of commercially pure aluminium [7] at room temperature.

A computer analysis of the results gave 'better-fitting' curves in the form of third order polynomial expressions

$$Y = A + BX + CX^2 + DX^3 \qquad (5)$$

where $Y = \log \gamma_t$ and $X = \log N_f$

The constants A, B, C, D are obviously temperature dependent and their values are plotted in Fig. 10.

Estimates of γ_t for a given life were predicted for specimens at 250 °C by extrapolating data from Fig. 10. Two tests at this highest temperature gave errors of zero and 3·5%.

The effect of temperature is to increase the fracture ductility for a specific life in terms of number of cycles to failure. This is also true for $N_f = \frac{1}{4}$ (monotonic torsion tests to failure) see Fig. 2. It was decided therefore to compensate for this increase in ductility above room temperature (20 °C) by introducing a correction factor β where

$$\beta = (\gamma_t)_{20°C} / (\gamma_t)_T \qquad (6)$$

For a given life, plots of β against temperature are straight lines and

$$\beta = 1 - m\,(T - 20) \qquad (7)$$

where m is a function of the number of cycles to failure, see Fig. 11.

From Fig. 11 and equation 7 one can determine the ductility correction factor β for a required life at any temperature in the range of

$$0{\cdot}57\ T_m > T > 0{\cdot}314\ T_m$$

Using this technique and plotting the compensated total plastic strain path to failure, $\beta\gamma_t$, against the logarithm of life all results from this investigation fall within a scatter band of ±4%, see Fig. 12. The curve in Fig. 12 can be described by the equation

$$N_f^{\alpha} = Ke^{\beta\gamma_t} \qquad (8)$$

Considering the various degrees of interaction between the various deformation processes recorded in this paper such a result, however empirical, seems to indicate that the total plastic strain path is a criterion of failure and this parameter should be corrected for changes in fracture ductility due to changes in temperature.

Conclusions

1. The rate of deformation affects the ratio of time-dependent to cyclic dependent deformation processes in high-strain fatigue. In consequence the number of cycles to failure and the cumulative strain are both strain rate dependent.
2. Time and cyclic processes are also dependent on torque range and temperature.
3. Above a critical straining rate $\dot{\gamma}_{crit}$ there is no significant effect on the number of cycles to failure. Below the critical rate the cyclically induced creep component becomes increasingly important as the strain rate decreases.
4. A critical torque range T_{crit} exists below which initial cyclic hardening occurs rather than the cyclic softening, experienced at $T > T_{crit}$.
5. Increasing temperature causes an increase in the value of $\dot{\gamma}_{crit}$ and a decrease in the value of T_{crit}.

6. At very low strain rates and high torque ranges, cyclic stress relaxation becomes more pronounced.

7. Irrespective of the degree of interaction between cyclic softening, cyclic hardening, stress relaxation and monotonic work hardening, the total plastic strain path, γ_t, provides a simple criterion of failure for any given temperature.

8. By introducing a fracture ductility correction factor, β, that is temperature and life dependent, all results of this investigation can be described by a single equation.

$$N_f = Ke^{\beta\gamma_t}$$

References

1. TILLY, G. P., *Nat. Gas Turbine Estab. Rep. (R278)*, 1966.
2. RARATY, L. E. & SUHR, R. W., *J. Inst. Metals*, vol. 94, p. 292, 1966.
3. DAVIES, V. de L. & BAKKEN, K., *J. Nuclear Mat.*, vol. 18, p. 226, 1966.
4. MILLER, K. J., 'International Conference on Thermal and High Strain Fatigue,' *Inst. of Metals*, London, p. 225, 1967.
5. MILLER, K. J., *Nature*, vol. 213, p. 317, 1967.
6. MILLER, K. J., 'The effect of specimen geometry on high strain fatigue behaviour', 4th Congress Materials, Testing, Budapest, 1967.
7. MILLER, K. J. & RIZK, M. N., *J. Strain Analysis*, October, 1968.
8. BENHAM, P. P. & FORD, H., *J. Mech. Eng. Sci.*, vol. 3, p. 119, 1961.

Table 1

Temperature °C	20	110	160	205
Critical strain rate $\times 10^4$s.	55·5	195	290	395

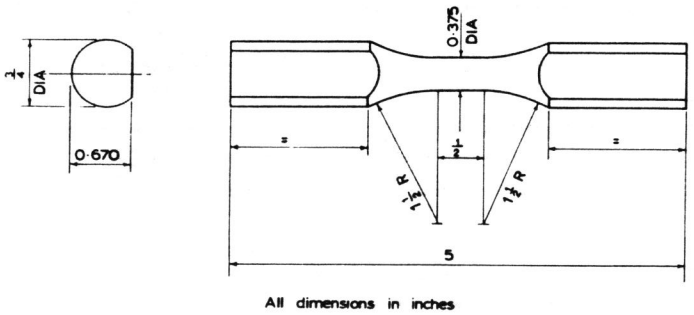

Fig. 1. Specimen geometry.

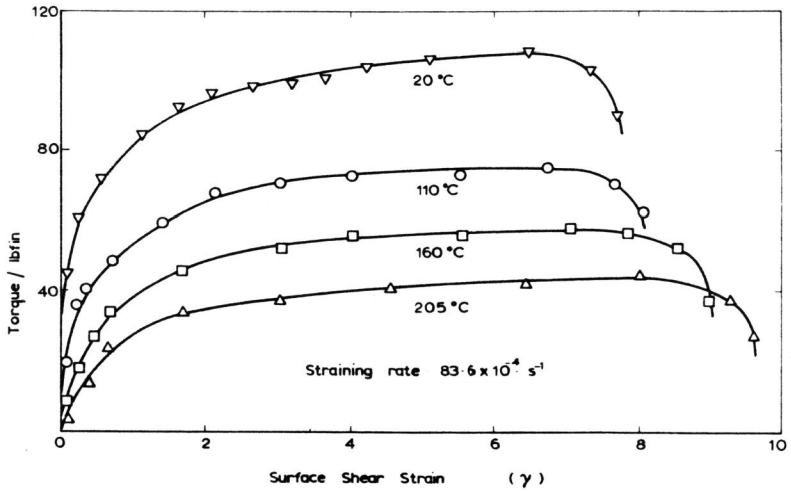

Fig. 2. Monotonic torsion test to fracture curves at various temperatures but constant straining rate.

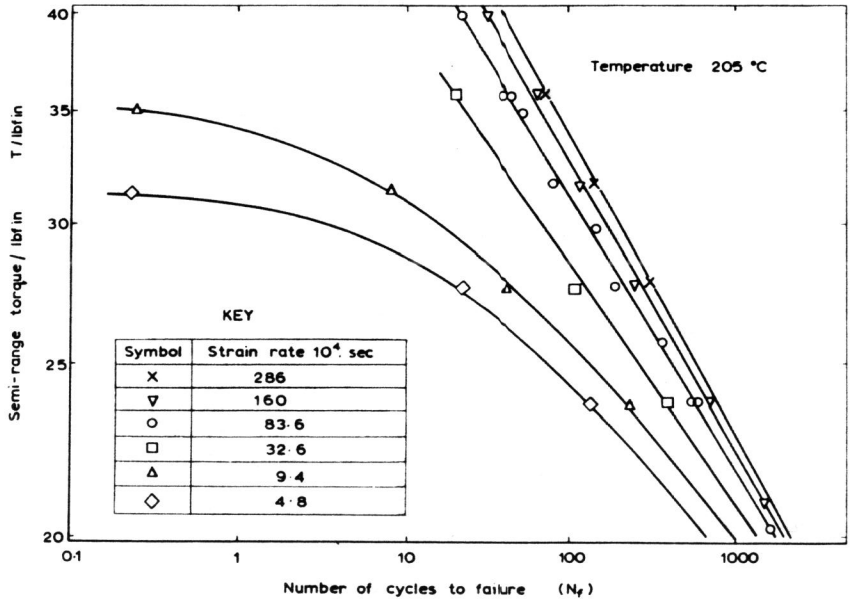

Fig. 3. A typical family of fatigue endurance curves.

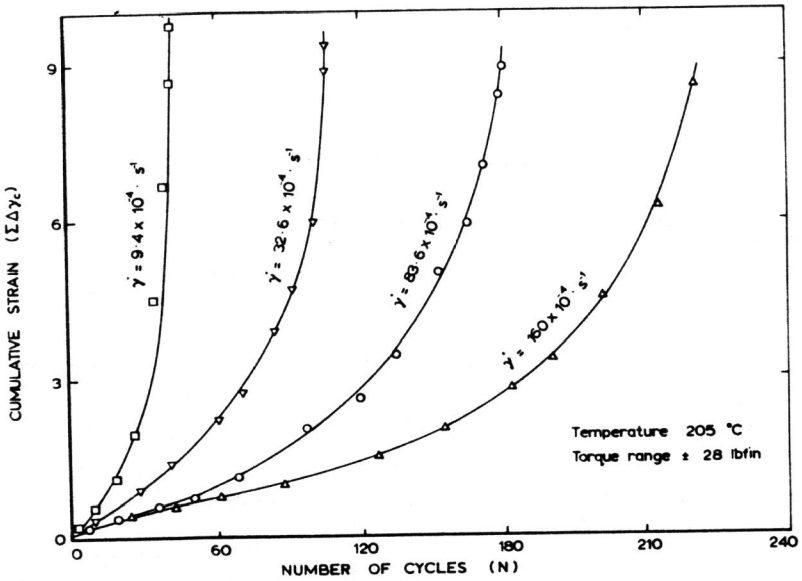

Fig. 4. A typical family of cyclically-induced-creep curves.

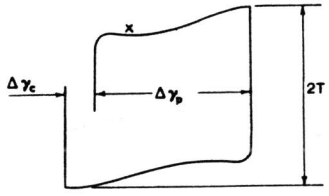

Fig. 5a. A hysteresis loop profile.

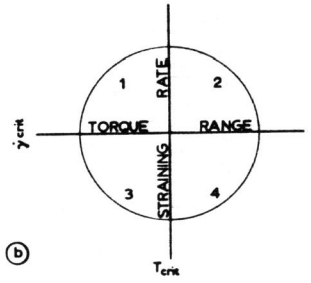

Fig. 5b. The four zones of deformation behaviour.

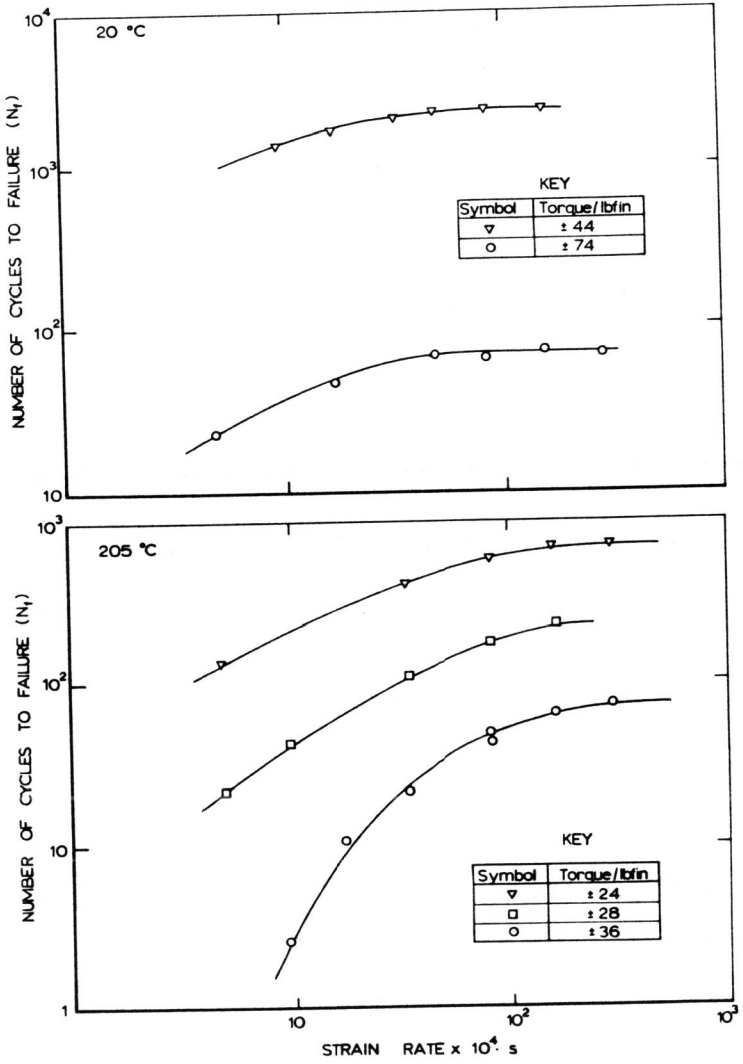

Fig. 6. The effect of strain rate, temperature and torque range on fatigue life.

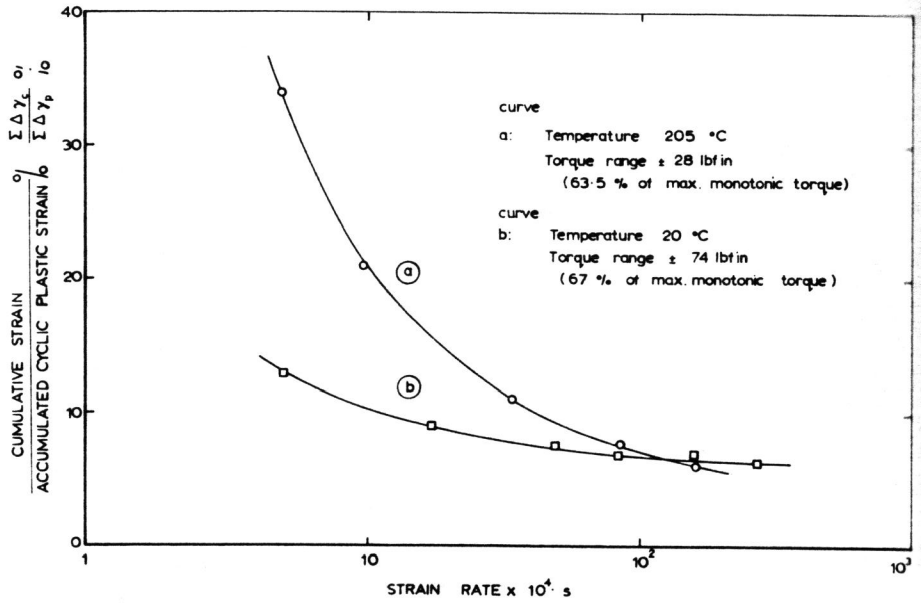

Fig. 7. The effect of temperature and strain rate on ratio, R.

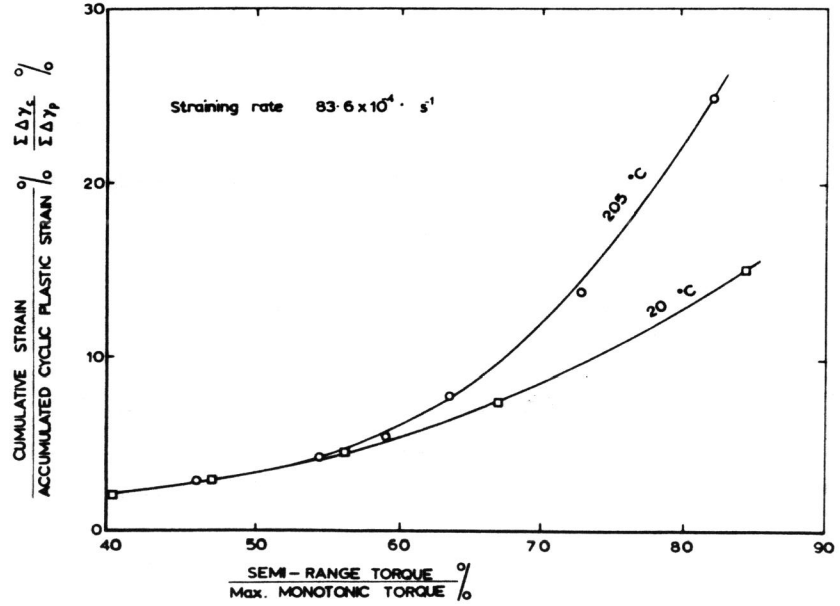

Fig. 8. The effect of torque range and temperature on the ratio, R.

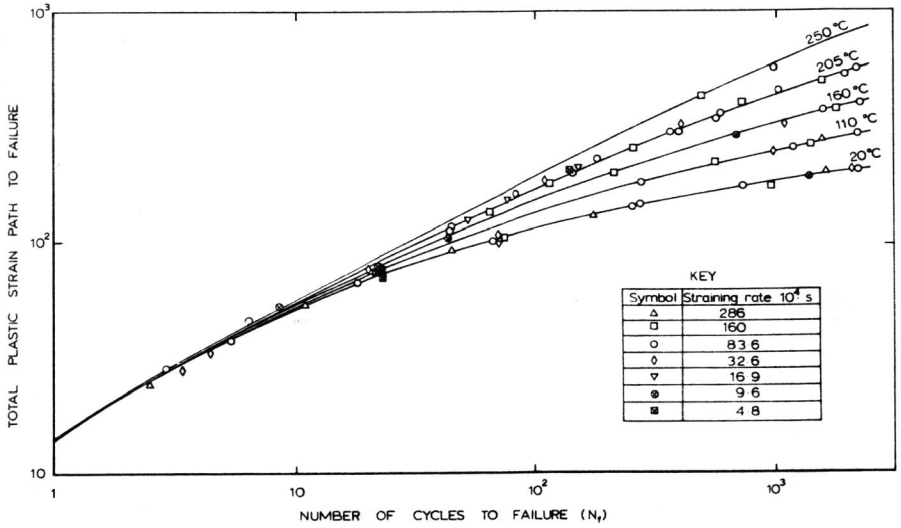

Fig. 9. The effect of temperature on the total plastic strain path criterion of failure.

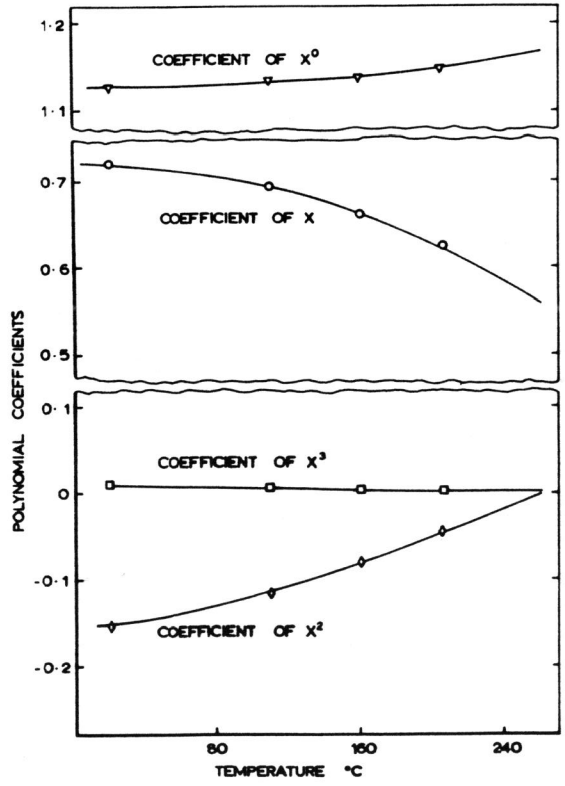

Fig. 10. The effect of temperature on the coefficients of the polynomial expression given in equation 5.

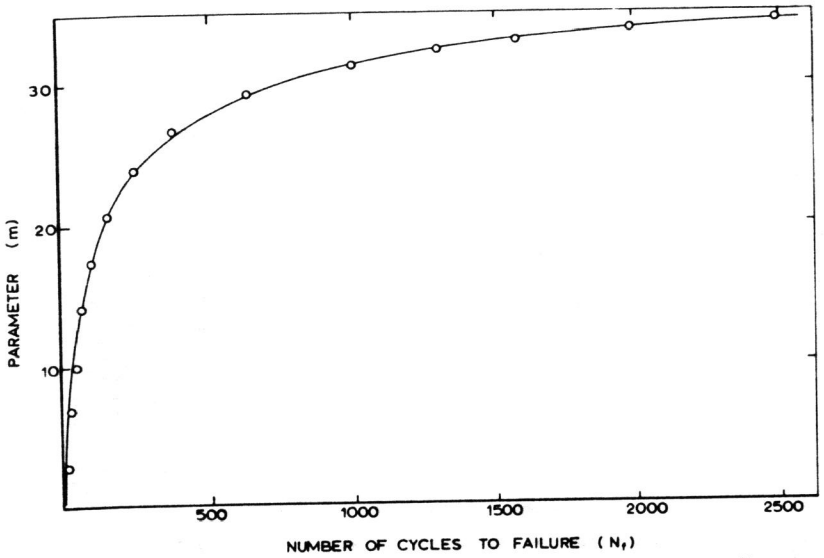

Fig. 11. The effect of life on the parameter m given in equation 7.

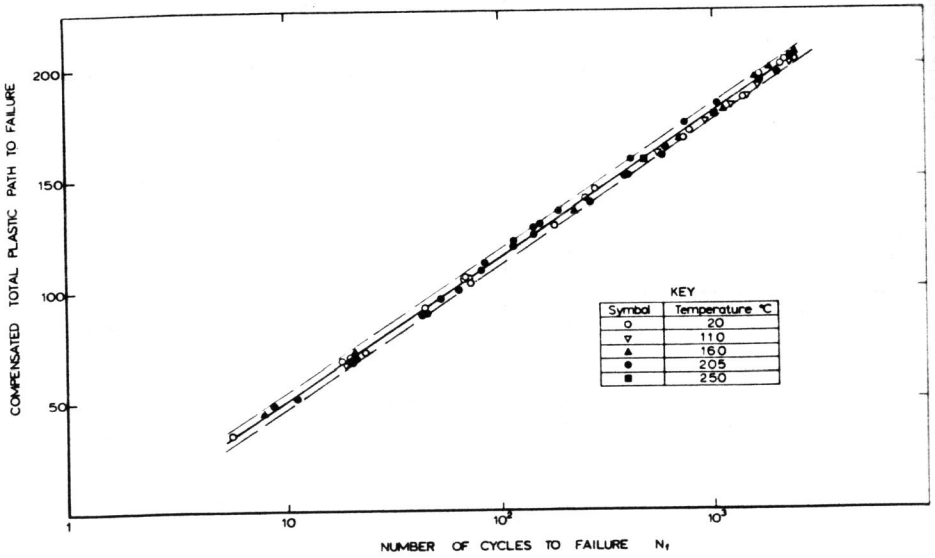

Fig. 12. A temperature compensated fatigue curve expressing all results of the investigation.